using a well-characterized polyclonal antibody against Herp, diluted 1 : 100 (Kokame *et al.* 2000). Double-immunofluorescence utilized an antibody against Herp combined with one of the following: (i) mouse monoclonal antibody 6E10 (Signet, Dedham, MA, USA), diluted 1 : 100, which morphologically recognizes Aβ in both AD brain (Kim *et al.* 1990) and s-IBM muscle (Askanas *et al.* 2000); (ii) mouse monoclonal antibody recognizing BiP/GRP78 (BD Transduction Laboratories, San Diego, CA, USA) diluted 1 : 20; (iii) mouse monoclonal antibody recognizing 20S proteasomal subunit β2 (Affinity Research Products Ltd, UK) diluted 1 : 50; (iv) mouse monoclonal antibody recognizing ubiquitin (Santa Cruz Biotechnology, Santa Cruz, CA, USA) diluted 1 : 50.

To block non-specific binding of antibody to Fc receptors, sections were pre-incubated with normal goat or rabbit serum diluted 1 : 10, as described (Askanas *et al.* 1993a, 2000). Controls for staining specificity were (i) omission of the primary antibody or (ii) its replacement with non-immune sera or irrelevant antibody.

Immuno-electronmicroscopy

Double-label gold immuno-electronmicroscopy was performed on 10-μm unfixed frozen biopsy sections adhered to the bottom of 35-mm Petri dishes, as detailed (Askanas *et al.* 1993a, 1996a, 2000). In brief, a primary antibody against Herp was used in combination with an antibody against Aβ, 20S proteasome, or BiP/GRP78. After incubation with the appropriate secondary antibodies conjugated to 5 nm and 15 nm gold particles, sections were processed for electronmicroscopy as described (Askanas *et al.* 1993a, 1996a, 2000).

Immunoblotting

Muscle biopsies of seven s-IBM and seven age-matched control patients were immunoblotted, as recently detailed (Vattemi *et al.* 2003, 2004). Briefly, 10-μm-thick frozen sections were collected in ristocetin-induced platelet agglutination (RIPA) buffer (50 mM Tris-HCl pH 8.0, 150 mM NaCl, 1 mM EDTA, 1% NP-40, 0.25% Na-deoxycholate, 0.1% sodium dodecyl sulfate) containing phenylmethylsulfonyl fluoride and protease inhibitor cocktail (Roche Diagnostic, Mannheim, Germany). All samples were rapidly homogenized on ice. Protein concentration was measured using the Bradford method (Vattemi *et al.* 2004): 20 μg of protein were loaded onto 10% NuPAGE gels (Invitrogen, Carlsbad, CA, USA), electrophoresed, transferred to nitrocellulose membranes, and immuno-probed with antibodies against Herp. After incubation in the appropriate secondary antibodies, blots were developed using an enhanced chemiluminescence system (ECL) (Amersham Biosciences, Piscataway, NJ, USA). Protein loading was evaluated by the actin band visualized with a mouse monoclonal antibody (Santa Cruz Biotechnology). Quantification of the immunoreactivity was performed by densitometric analysis using NIH Image J 1.310 software.

RNA isolation and reverse transcription–polymerase chain reaction

Total RNA from 10-μm-thick frozen sections of s-IBM and control muscle biopsies was isolated using an RNA isolation kit (BD Pharmingen, San Diego, CA, USA) according to the manufacturer's instructions. RNA samples were treated with Dnase I (Amplification Grade, Invitrogen) and 1 μg of RNA was submitted for cDNA synthesis using an oligo-dT primer (Invitrogen) and the Omniscript RT kit (Qiagen, Valencia, CA, USA). Then 1/10 of the RT reaction was amplified using multiplex PCR in a total volume of 20 μL, with Platinum Taq DNA Polymerase (Invitrogen), utilizing previously described primers for Herp (Kokame *et al.* 2000) and for glyceraldehyde-3-phosphate dehydrogenase (GAPDH) (Lehmann *et al.* 2002) as an internal control. The optimized conditions for Herp and GAPDH amplification were 2 min at 94°C followed by 28 cycles of amplification (94°C for 30 s, 60°C for 30 s, 72°C for 90 s), and the final incubation was 10 min at 72°C. The PCR products were separated on a 2% agarose gel and stained with ethidium bromide. The conditions of the reactions were experimentally checked to ensure that signals were in the linear range of the PCR. Identity of the products was confirmed by sequencing.

Statistical analysis

The statistical significance of differences between groups was determined by Student's *t*-test. The level of significance was set at $p < 0.05$. Data are presented as means ± SEM for all groups.

Cultured human muscle fibers

Primary cultures of normal human muscle were established from satellite cells of portions of diagnostic muscle biopsies from patients who, after all tests were performed, were considered free of muscle disease (Askanas and Engel 1992; Askanas *et al.* 1996b). Experiments were performed on seven culture sets, each established from a different muscle biopsy. All experimental conditions were studied on sister cultures in the same culture sets. Three-week-old cultured muscle fibers were treated for 24 h with either (i) one of two well-known ER stress inducers, N-glycosylation inhibitor tunicamycin (4 μg/mL) or an inhibitor of ER-calcium-ATPase thapsigargin (300 nM) (Back *et al.* 2005; Lee 2005) (both from Sigma Co, St. Louis, MO, USA) or (ii) epoxomicin (1 μM) (Biomol Research Laboratories, Plymouth Meeting, PA, USA), a specific and irreversible proteasome inhibitor (Meng *et al.* 1999). After treatment, control and experimental cultures were fixed for immunostainings, harvested for immunoblot studies, or used for RNA isolation.

Light-microscopic immunocytochemistry

Single and double immunofluorescence on paraformaldehyde-fixed cultures was performed as described (Askanas *et al.* 1996b, 1997; Fratta *et al.* 2005).

Immunoblotting

Cultured cells were harvested in ristocetin-induced platelet agglutination (RIPA) buffer containing phenylmethylsulfonyl fluoride and a protease inhibitor cocktail (Roche Diagnostic). The immunoblotting procedure was performed as described above for muscle biopsies.

Reverse transcription–polymerase chain reaction and northern blots

Total RNA from control and experimental cultures was extracted using RNA-bee reagent (Tel Tech, Friendwood, TX, USA). After treatment with Dnase I, 150 ng of RNA was used for one-step synthesis of cDNA and the multiplex PCR reaction (Qiagen). The optimized conditions were 30 min at 50°C, 15 min at 95°C

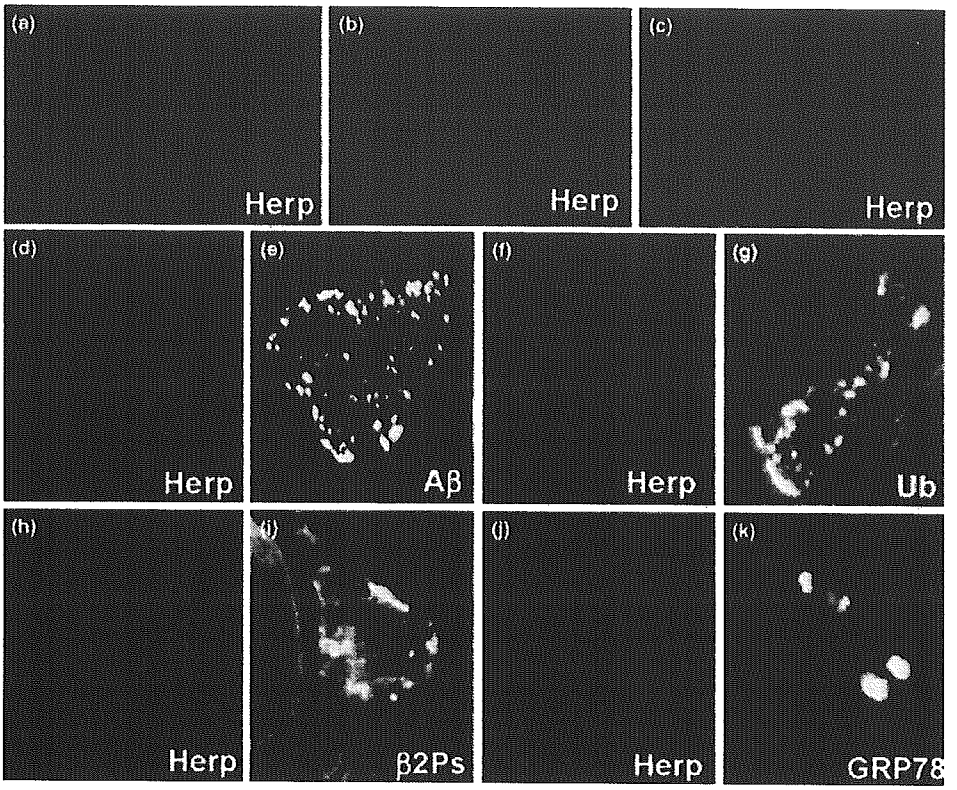

Fig. 1 Immunofluorescence within sporadic inclusion-body myositis muscle fibers. (a–c) Single-label immunofluorescence illustrates immunoreactivity of homocysteine-induced endoplasmic reticulum protein (Herp) in the form of various-sized aggregates. Double-label immunofluorescence illustrates that Herp immunoreactive inclusions (d, f, h, j) co-localized with amyloid-β (Aβ) (e), ubiquitin (g), β2 20S proteasome subunit (i), and Bip/GRP78 ER chaperone (k). Magnification: a–c, f–k, ×1100; d, e ×700. BiP/GRP78, immunoglobulin heavy chain-binding protein/glucose-regulated protein 78; β2Ps, β2 20S proteasome subunit; Ub, ubiquitin.

followed by 28 cycles of amplification (94°C for 30 s, 60°C for 30 s, 72°C for 90 s), and the final incubation of 10 min at 72°C.

For northern blots, aliquots of RNA (10 μg) isolated from experimental and control cultures were denatured and subjected to electrophoresis in 1% agarose gel containing 0.41 M formaldehyde. After electropheretic fractionation, RNA was transferred overnight to a positively charged nylon membrane by capillary blotting and fixed by UV light. A Herp-specific probe was generated by PCR and fluorescein-labelled (Kokame *et al.* 2000). Hybridization and detection procedures using anti-fluorescein-AP conjugate were performed as described (Kokame *et al.* 2000).

Statistical analysis

The statistical analysis was as described above.

Results

Muscle biopsies

Light-microscopic immunocytochemistry

In all s-IBM muscle biopsies, 70–80% of the vacuolated muscle fibers contained, mainly in their non-vacuolated cytoplasm, numerous various-sized aggregates immunoreactive with antibodies against Herp (Figs 1a–c). Approximately 25% of non-vacuolated muscle fibers also contained similar aggregates. By double immunofluorescence, Herp immunoreactive aggregates co-localized with Aβ (Figs 1d and e), ubiquitin (Figs 1f and g), β2 proteasome subunit (Figs 1h and i), and BiP/GRP78 (Figs 1j and k). None of the control non-s-IBM, diseased or normal, human muscle biopsies had muscle fibers containing aggregates immunoreactive with anti-Herp antibody. Eliminating the primary antibodies or replacing them with non-relevant antibodies resulted in non-staining.

Gold-immuno-electronmicroscopy

Immunoreactive Herp was associated with Aβ, 20S β2 proteasome subunit, and BiP/GRP78 within the same structures, namely the 6–10 nm fibrils and amorphous and floccular material (Fig. 2). Herp was not associated with paired helical filaments, which are known to contain phosphorylated tau in IBM muscle fibers (Mirabella *et al.* 1996).

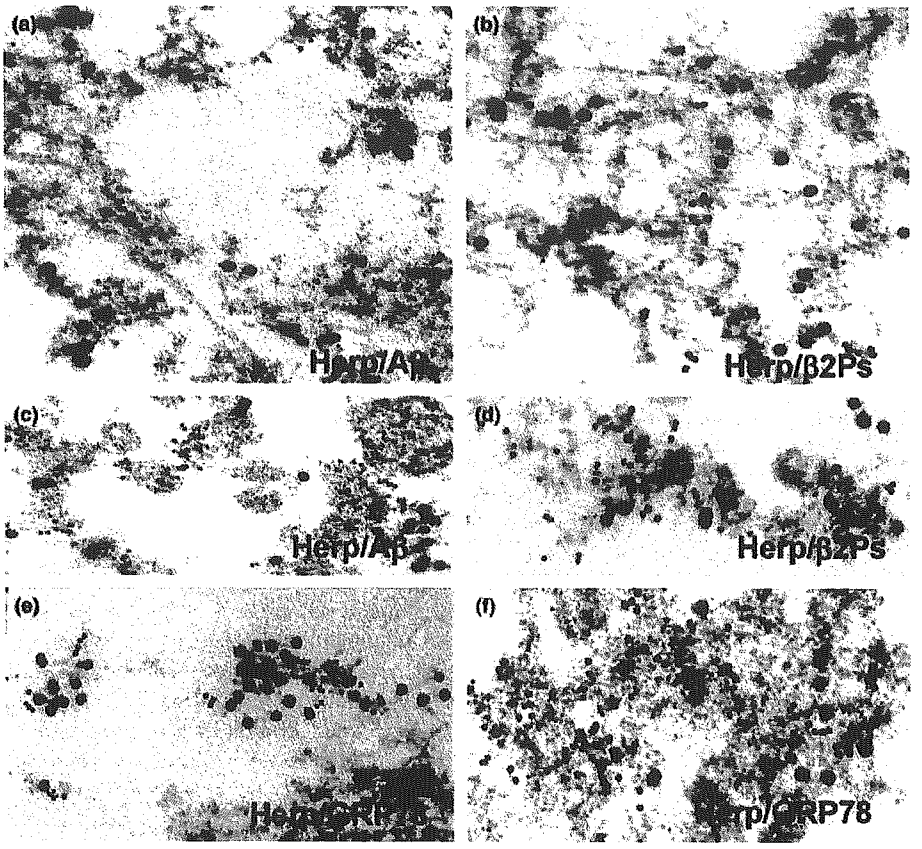

Fig. 2 Double-label gold-immuno-electronmicroscopy in sporadic inclusion-body myositis muscle fibers. This illustrates that both homocysteine-induced endoplasmic reticulum protein (Herp) (5 nm gold particles) and amyloid-β (Aβ) (15 nm gold particles) are associated with 6–10 nm fibrils (a) and floccular material (c). Similarly, Herp (5 nm gold) and β2 20S proteasome subunit (15 nm gold) (b, d) and Herp (5 nm gold) and BiP/GRP78 (15 nm gold) (e, f) are associated with the same 6–10 nm fibrils and floccular material. Magnification: a, c–f, ×51 000; b, ×60 000. BiP/GRP78, immunoglobulin heavy chain-binding protein/glucose-regulated protein 78; β2Ps, β2 20S proteasome subunit; Ub, ubiquitin.

Immunoblots

In normal and s-IBM muscle, Herp migrated as a single 54 kDa band (Fig. 3a), and its expression was much stronger in s-IBM muscle as compared to controls. Omission of the primary antibody resulted in no bands being present (Fig. 3b). Figure 3(c) provides analysis of the data derived from densitometric scans (obtained from seven samples), normalized to β-actin and expressed in arbitrary units. These data indicate that in s-IBM muscle biopsies Herp protein was increased eight-fold ($p < 0.05$) as compared to controls.

RNA expression by reverse transcription–polymerase chain reaction

As determined by RT–PCR analysis, Herp mRNA was prominently increased in s-IBM as compared to controls (Figs 3d and e).

Cultured human muscle fibers

Light-microscopic immunocytochemistry

In control fibers, Herp immunoreactivity was only weak and diffuse (Fig. 4a). ER stress-induced cultured human muscle fibers had strong and diffuse Herp immunoreactivity (Figs 4b and c). In contrast, approximately 80% of the epoxomicin-treated muscle fibers had the Herp protein immunoreactivity in the form of large aggregates (Figs 4d, e, and g), which co-localized with ubiquitin immunoreactivity (Figs 4f and h).

Immunoblots

Treatment with ER-stress inducers or with epoxomicin prominently increased the Herp protein level as illustrated by two representative culture sets (Fig. 5a). Figure 5(b) provides densitometric analysis of the data from seven

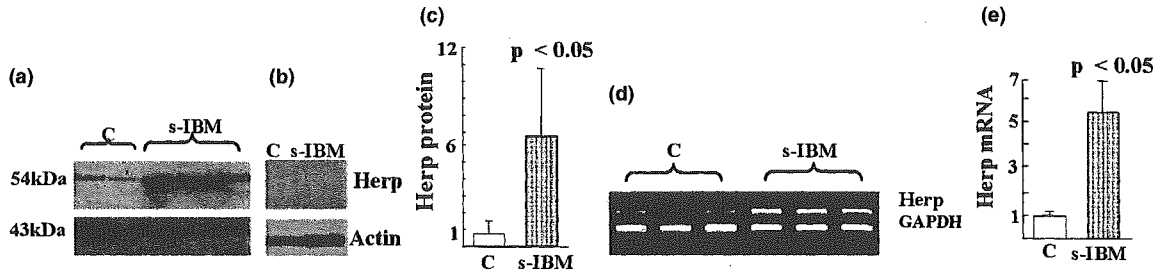

Fig. 3 Immunoblots and RT–PCR in control and sporadic inclusion-body myositis (s-IBM) samples. (a) Immunoblots of muscle homogenates of normal-control (C) and s-IBM muscle biopsies demonstrate much stronger expression of homocysteine-induced endoplasmic reticulum protein (Herp) in s-IBM. The actin bands indicate protein loading in each sample. (b) Omission of the primary anti-Herp antibody resulted in no bands. (c) Densitometric analysis of the blots performed using NIH Image J 1.310 indicates that in s-IBM muscle biopsies Herp protein was eight-fold increased as compared to controls. Data are indicated as mean ± SEM. Significance was determined by *t*-test. The level of significance was set at $p < 0.05$. (d) Representative agarose gel electrophoresis of products corresponding to Herp and glyceraldehyde-3-phosphate dehydrogenase (GAPDH), amplified by the Multiplex PCR method. (e) Densitometric analysis of the PCR bands, expressed in arbitrary units, indicates that Herp mRNA is increased in s-IBM muscle fibers. The GAPDH mRNA was used to normalize corresponding Herp results.

experimental sets, normalized to β-actin. Thapsigargin, the strongest Herp-inducer, increased Herp about 15-fold ($p < 0.01$). Tunicamycin and epoxomicin increased Herp six-fold ($p < 0.01$) and 10-fold ($p < 0.05$), respectively (Fig. 5b). In some thapsigargin, tunicamycin, or epoxomicin treated cultures, additional bands lower than 54 kDa were occasionally observed (not shown). This suggests, as shown previously in PC12 cells (Chan *et al.* 2004), that under certain experimental conditions, some cleavage of Herp can also occur in cultured muscle fibers.

Reverse transcription–polymerase chain reaction and northern blotting analysis

To investigate the molecular basis of Herp protein increase, semiquantitative multiplex RT–PCR analysis was performed. Those studies indicated in each experiment that thapsigargin and tunicamycin increased Herp mRNA, whereas epoxomicin appeared to slightly decrease it (Figs 5c and d). The above data were confirmed by northern blots (Fig. 5e).

Discussion

We investigated expression of Herp in normal and diseased human muscle, and studied the mechanisms of Herp regulation in cultured human muscle fibers. We report that in s-IBM muscle fibers, Herp was accumulated in various-sized multifocal aggregates, wherein it co-localized with Aβ, ER chaperone BiP/GRP78, and 20S β2 proteasome subunit, by both light- and electronmicroscopic immunocytochemistry.

In addition, Herp protein and its mRNA were prominently increased in s-IBM muscle fibers. Even though normal human muscle fibers had, on immunoblots, a definite band of Herp, neither in them nor in several non-s-IBM diseased human muscle biopsies was Herp discerned immunocytochemically by light-microscopy. Previous studies have shown Herp mRNA expression in various human organs, including skeletal muscle (Kokame *et al.* 2000), but they did not study Herp protein.

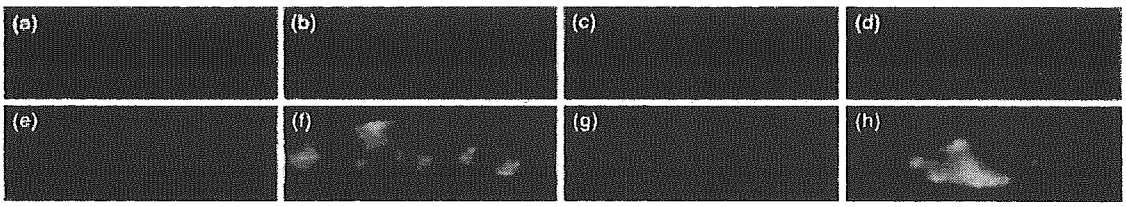

Fig. 4 Immunofluorescence in cultured human muscle fibers. Single-label immunofluorescence of homocysteine-induced endoplasmic reticulum protein (Herp) (a–d) shows very weak, barely detectable immunoreactivity in a control (a) cultured muscle fiber. Strong and diffuse immunoreactivity was present in cultures treated with endoplasmic reticulum (ER) stress inducers thapsigargin (b) and tunicamycin (c). In cultures treated with the proteasome inhibitor, epoxomicin, Herp immunoreactivity was in the form of large aggregates (d). Double-label immunofluorescence illustrates that in epoxomicin-treated cultures Herp immunoreactive aggregates (e, g) were also immunoreactive with an antibody against ubiquitin (f, h). Magnification: all ×1400.

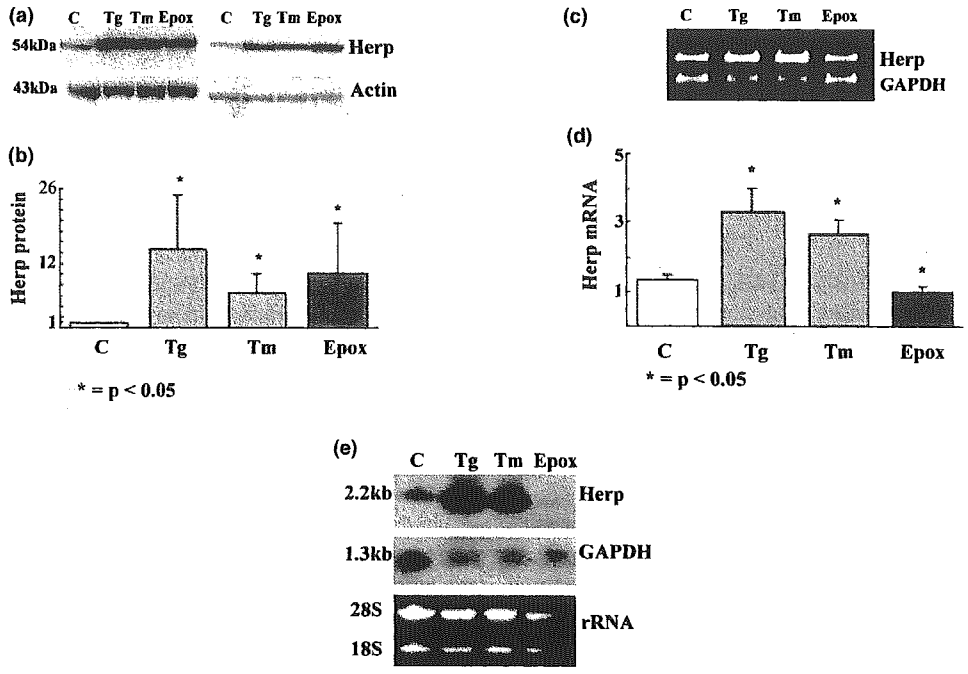

Fig. 5 Immunoblots, RT–PCR, and northern blotting in cultured human muscle fibers. (a) Immunoblots of two representative culture sets show the increase of homocysteine-induced endoplasmic reticulum protein (Herp) in thapsigargin (Tg), tunicamycin (Tm), and epoxomicin (Epox) treated cultured human muscle fibers as compared to controls (C). (b) Densitometric analysis of blots in (a), analyzed using NIH Image J 1.310, shows that thapsigargin, tunicamycin, and epoxomicin prominently increased Herp protein. Data were obtained from seven independent experimental sets of cultured human muscle, and are presented as the mean ± SEM of fold increase. Significance was determined by *t*-test. The level of significance was set at $p < 0.05$. (c) Representative agarose gel electrophoresis of products corresponding to Herp and glyceraldehyde-3-phosphate dehydrogenase (GAPDH), amplified by Multiplex PCR method. (d) Densitometric analysis of the PCR bands expressed in arbitrary units. The GAPDH mRNA was used to normalize corresponding Herp results. Those data show that thapsigargin and tunicamycin increased Herp mRNA, whereas epoxomicin appears to slightly decrease Herp mRNA. (e) Northern blotting of Herp mRNA in control (C), thapsigargin (Tg), tunicamycin (Tm), and epoxomicin (Epox) treated cultured human muscle fibers shows results similar to those obtained by PCR. GAPDH illustrates RNA loading, which corresponds to the 28S and 18S RNA visualized by staining of the agarose gel with ethidium bromide.

Our studies, based on experimentally modified cultured human muscle, demonstrated two distinct mechanisms of Herp increase in normal human muscle, and they seem directly relevant to s-IBM muscle fibers. Specifically, two ER-stress inducers, tunicamycin and thapsigargin, each increased Herp transcription and translation, which resulted in very strong and diffuse immunoreactivity of its protein. However, proteasome inhibition by epoxomicin increased the amount of Herp total protein without increasing its transcription, and produced striking aggregations of Herp, which, similarly to the s-IBM muscle biopsies, were associated with ubiquitin. As ER-stress and proteasome inhibition are present in s-IBM muscle fibers, we propose that those two mechanisms contribute to the demonstrated Herp abnormalities in s-IBM muscle fibers.

Even though Herp is considered the most inducible protein during ER-stress (Yamamoto *et al.* 2004), its exact relationship to the ER-stress is not well understood. Accumulation of unfolded/misfolded proteins in the ER induces ER-stress, which activates three pathways of the UPR, the role of which is to mitigate the ER-stress. One pathway involves preferential translation of transcription-factor ATF4 (Shen *et al.* 2004; Schroder and Kaufman 2005). The Herp promoter contains ER-stress-responsive elements, including a *cis*-acting element recognized by ATF4 (Ma and Hendershot 2004; Yamamoto *et al.* 2004). Our preliminary data (not shown) indicate that ATF4 is increased in s-IBM muscle fibers, suggesting that ATF4 may be involved in overexpression of Herp. Whether other transcription factors, such as ATF6 or X-box-binding protein 1 (XBP-1), participate in Herp induction in s-IBM muscle fibers and in our culture model is not known. Thus, the exact pathways that contribute to Herp activation in s-IBM muscle fibers remain to be studied.

The half-life of Herp is considered to be very short (2.5 h) (Sai *et al.* 2003). Its ubiquitin-like domain (ULD) is responsible for its rapid degradation via the 26S proteasome (Sai *et al.* 2003). Because 26S proteasome activity is

inhibited in s-IBM muscle fibers (Fratta *et al.* 2005), this inhibition may contribute to the total increase of Herp protein, as well as its accumulation in the form of ubiquitin-associated aggregates.

We have also shown other proteins accumulated and aggregated in s-IBM muscle fibers and in our proteasome-inhibited cultures of human muscle fibers (Fratta *et al.* 2005). As Herp was proposed to be linked to both UPR and ERAD (Yamamoto *et al.* 2004; Schroder and Kaufman 2005), its co-localization with BiP/GRP78, 20S proteasome, and Aβ in s-IBM muscle fibers might suggest that Herp in s-IBM is involved in attempted proper folding of proteins and in the pathway of proteasomal removal of improperly folded ones.

Herp has been previously shown to influence processing of amyloid-β precursor protein (AβPP) and Aβ production through its binding to presenilin 1 (Sai *et al.* 2002). Presenilin 1 is increased in s-IBM muscle fibers (Askanas *et al.* 1998), but our present studies did not address the question of whether Herp participates in AβPP processing and Aβ production in s-IBM muscle fibers or in our cultured human muscle fibers.

A role of Herp in preventing ER-stress-induced apoptotic cell death in non-muscle cells (Chan *et al.* 2004; Hori *et al.* 2004) is of interest regarding s-IBM muscle fibers. s-IBM fibers do not exhibit features of apoptosis (Behrens *et al.* 1997; Askanas and Engel 2001), despite intracellular existence of several factors, such as increased Aβ, oxidative stress, and mitochondrial abnormalities (Askanas and Engel 2001, 2003) known to induce apoptosis in other cells (Loo *et al.* 1993; Simonian and Coyle 1996; Parone *et al.* 2002). We have previously proposed that the multinucleated muscle fibers do not undergo classic apoptosis (Broccolini *et al.* 1999; Askanas and Engel 2001). In s-IBM muscle fibers, survival motor neuron (SMN) factor and IAP-like protein were previously proposed to play an anti-apoptotic role (Broccolini *et al.* 2000; Li and Dalakas 2000; Askanas and Engel 2001). Based on our current data, it is possible that Herp might also contribute to the anti-apoptotic milieu in s-IBM muscle fibers, as was shown in relation to other cells (Chan *et al.* 2004; Hori *et al.* 2004).

Conclusion

Our novel findings related to the increase of Herp and its abnormal multifocal accumulation in s-IBM muscle fibers are reported. We demonstrate, for the first time, that two different mechanisms are involved in Herp regulation and accumulation in human muscle fibers. We suggest that Herp, amelioratively, might be facilitating the unfolded protein response and attempting to enhance the ER-associated protein degradation of malfolded proteins in s-IBM muscle fibers. Nevertheless, despite the existence in the s-IBM muscle fibers of Herp and components of the unfolded protein response that are putatively protective, s-IBM is a severely progressive degenerative disease, probably because the factors causing progressive degeneration are more influential than those having a putative protective influence. Accordingly, developing methods that would further up-regulate the protective factors might lead to novel therapeutic avenues.

Acknowledgements

Supported by grants from the National Institutes of Health (AG16768 Merit Award), the Myositis Association, the Muscular Dystrophy Association (to VA), and the Helen Lewis Research Fund. Maggie Baburyan provided excellent technical assistance in electronmicroscopy.

References

Askanas V. and Engel W. K. (1992) Cultured normal and genetically abnormal human muscle, in *The Handbook of Clinical Neurology, Myopathies*, Vol. 18 (Rowland L. P. and Di Mauro S., eds), pp. 85–116. North Holland, Amsterdam.

Askanas V. and Engel W. K. (2001) Inclusion-body myositis: newest concepts of pathogenesis and relation to aging and Alzheimer disease. *J. Neuropathol. Exp. Neurol.* **60**, 1–14.

Askanas V. and Engel W. K. (2002) Inclusion-body myositis and myopathies: different etiologies, possibly similar pathogenic mechanisms. *Curr. Opin. Neurol.* **15**, 525–531.

Askanas V. and Engel W. K. (2003) Proposed pathogenetic cascade of inclusion-body myositis: importance of amyloid-beta, misfolded proteins, predisposing genes, and aging. *Curr. Opin. Rheumatol.* **15**, 737–744.

Askanas V., Alvarez R. B. and Engel W. K. (1993a) Beta-amyloid precursor epitopes in muscle fibers of inclusion body myositis. *Ann. Neurol.* **34**, 551–560.

Askanas V., Engel W. K. and Alvarez R. B. (1993b) Enhanced detection of congo-red-positive amyloid deposits in muscle fibers of inclusion body myositis and brain of Alzheimer's disease using fluorescence technique. *Neurology* **43**, 1265–1267.

Askanas V., Alvarez R. B., Mirabella M. and Engel W. K. (1996a) Use of anti-neurofilament antibody to identify paired-helical filaments in inclusion-body myositis. *Ann. Neurol.* **39**, 389–391.

Askanas V., McFerrin J., Baque S., Alvarez R. B., Sarkozi E. and Engel W. K. (1996b) Transfer of beta-amyloid precursor protein gene using adenovirus vector causes mitochondrial abnormalities in cultured normal human muscle. *Proc. Natl Acad. Sci. USA* **93**, 1314–1319.

Askanas V., McFerrin J., Alvarez R. B., Baque S. and Engel W. K. (1997) Beta APP gene transfer into cultured human muscle induces inclusion-body myositis aspects. *Neuroreport* **8**, 2155–2158.

Askanas V., Engel W. K., Yang C. C., Alvarez R. B., Lee V. M. and Wisniewski T. (1998) Light and electron microscopic immunolocalization of presenilin 1 in abnormal muscle fibers of patients with sporadic inclusion-body myositis and autosomal-recessive inclusion-body myopathy. *Am. J. Pathol.* **152**, 889–895.

Askanas V., Engel W. K., Alvarez R. B., McFerrin J. and Broccolini A. (2000) Novel immunolocalization of alpha-synuclein in human muscle of inclusion-body myositis, regenerating and necrotic muscle fibers, and at neuromuscular junctions. *J. Neuropathol. Exp. Neurol.* **59**, 592–598.

Back S. H., Schröoder M., Lee K., Zhang K. and Kaufman R. J. (2005) ER stress signaling by regulated splicing: IRE1/HAC1/XBP1. *Methods* **35**, 395–416.

Behrens L., Bender A., Johnson M. A. and Hohlfeld R. (1997) Cytotoxic mechanisms in inflammatory myopathies. Co-expression of Fas and protective Bcl-2 in muscle fibres and inflammatory cells. *Brain* **120**, 929–938.

Borden K. L. (1998) Structure/function in neuroprotection and apoptosis. *Ann. Neurol.* **44**, S65–S71.

Broccolini A., Engel W. K. and Askanas V. (1999) Localization of survival motor neuron protein in human apoptotic-like and regenerating muscle fibers, and neuromuscular junctions. *Neuroreport* **10**, 1637–1641.

Broccolini A., Engel W. K., Alvarez R. B. and Askanas V. (2000) Paired helical filaments of inclusion-body myositis muscle contain RNA and survival motor neuron protein. *Am. J. Pathol* **156**, 1151–1155.

Chan S. L., Fu W., Zhang P., Cheng A., Lee J., Kokame K. and Mattson M. P. (2004) Herp stabilizes neuronal Ca2+ homeostasis and mitochondrial function during endoplasmic reticulum stress. *J. Biol. Chem.* **279**, 28 733–28 743.

Cuello A. C. (2005) Intracellular and extracellular Abeta, a tale of two neuropathologies. *Brain Pathol.* **15**, 66–71.

Ellgaard L. and Helenius A. (2001) ER quality control: towards an understanding at the molecular level. *Curr. Opin. Cell Biol.* **13**, 431–437.

Engel W. K. and Cunningham G. G. (1963) Rapid examination of muscle tissue and improved trichrome method for fresh-frozen biopsy sections. *Neurology* **13**, 919–923.

Fratta P., Engel W. K., McFerrin J., Davies K. J., Lin S. W. and Askanas V. (2005) Proteasome inhibition and aggresome formation in sporadic inclusion-body myositis and in amyloid-{beta} precursor protein-overexpressing cultured human muscle fibers. *Am. J. Pathol.* **167**, 517–526.

Hori O., Ichinoda F., Yamaguchi A. *et al.* (2004) Role of Herp in the endoplasmic reticulum stress response. *Genes Cells* **9**, 457–469.

Kaufman R. J. (1999) Stress signaling from the lumen of the endoplasmic reticulum: coordination of gene transcriptional and translational controls. *Genes Dev.* **13**, 1211–1233.

Kim K. S., Wen G. Y., Bancher C., Chen J., Sapienza V., Hong H. and Wisniewski H. M. (1990) Detection and quantitation of amyloid B-peptide with 2 monoclonal antibodies. *Neurosci. Res. Commun.* **7**, 113–122.

Kokame K., Agarwala K. L., Kato H. and Miyata T. (2000) Herp, a new ubiquitin-like membrane protein induced by endoplasmic reticulum stress. *J. Biol. Chem.* **275**, 32 846–32 853.

Lee A. S. (2005) The ER chaperone and signaling regulator GRP78/BiP as a monitor of endoplasmic reticulum stress. *Methods* **35**, 373–381.

Lehmann M. H., Weber J., Gastmann O. and Sigusch H. H. (2002) Pseudogene-free amplification of human GAPDH cDNA. *Biotechniques* **33**, 769–770.

Li M. and Dalakas M. C. (2000) Expression of human IAP-like protein in skeletal muscle: a possible explanation for the rare incidence of muscle fiber apoptosis in T-cell mediated inflammatory myopathies. *J. Neuroimmunol.* **106**, 1–5.

Liu C. Y. and Kaufman R. J. (2003) The unfolded protein response. *J. Cell Sci.* **116**, 1861–1862.

Loo D. T., Copani A., Pike C. J., Whittemore E. R., Walencewicz A. J. and Cotman C. W. (1993) Apoptosis is induced by beta-amyloid in cultured central nervous system neurons. *Proc. Natl Acad. Sci. USA* **90**, 7951–7955.

Ma Y. and Hendershot L. M. (2004) Herp is dually regulated by both the endoplasmic reticulum stress-specific branch of the unfolded protein response and a branch that is shared with other cellular stress pathways. *J. Biol. Chem.* **279**, 13 792–13 799.

Meng L., Mohan R., Kwok B. H., Elofsson M., Sin N. and Crews C. M. (1999) Epoxomicin, a potent and selective proteasome inhibitor, exhibits in vivo antiinflammatory activity. *Proc. Natl Acad. Sci. USA* **96**, 10 403–10 408.

Mirabella M., Alvarez R. B., Bilak M., Engel W. K. and Askanas V. (1996) Difference in expression of phosphorylated tau epitopes between sporadic inclusion-body myositis and hereditary inclusion-body myopathy. *J. Neuropathol. Exp. Neurol.* **55**, 774–786.

Mori K. (2000) Tripartite management of unfolded proteins in the endoplasmic reticulum. *Cell* **101**, 451–454.

Parone P. A., James D. and Martinou J. C. (2002) Mitochondria: regulating the inevitable. *Biochimie* **84**, 105–111.

Rutkowski D. T. and Kaufman R. J. (2004) A trip to the ER: coping with stress. *Trends Cell Biol.* **14**, 20–28.

Sai X., Kawamura Y., Kokame K. *et al.* (2002) Endoplasmic reticulum stress-inducible protein, Herp, enhances presenilin-mediated generation of amyloid beta-protein. *J. Biol. Chem.* **277**, 12 915–12 920.

Sai X., Kokame K., Shiraishi H., Kawamura Y., Miyata T., Yanagisawa K. and Komano H. (2003) The ubiquitin-like domain of Herp is involved in Herp degradation, but not necessary for its enhancement of amyloid beta-protein generation. *FEBS Lett.* **553**, 151–156.

Schroder M. and Kaufman R. J. (2005) The mammalian unfolded protein response. *Annu. Rev. Biochem.* **74**, 739–789.

Selkoe D. J. (2001) Alzheimer's disease: genes, proteins, and therapy. *Physiol. Rev.* **81**, 741–766.

Shen X., Zhang K. and Kaufman R. J. (2004) The unfolded protein response-a stress signaling pathway of the endoplasmic reticulum. *J. Chem. Neuroanat.* **28**, 79–92.

Simonian N. A. and Coyle J. T. (1996) Oxidative stress in neurodegenerative diseases. *Annu. Rev. Pharmacol. Toxicol.* **36**, 83–106.

Travers K. J., Patil C. K., Wodicka L., Lockhart D. J., Weissman J. S. and Walter P. (2000) Functional and genomic analyses reveal an essential coordination between the unfolded protein response and ER-associated degradation. *Cell* **101**, 249–258.

Vattemi G., Engel W. K., McFerrin J. and Askanas V. (2003) Cystatin C colocalizes with amyloid-beta and coimmunoprecipitates with amyloid-beta precursor protein in sporadic inclusion-body myositis muscles. *J. Neurochem.* **85**, 1539–1546.

Vattemi G., Engel W. K., McFerrin J. and Askanas V. (2004) Endoplasmic reticulum stress and unfolded protein response in inclusion body myositis muscle. *Am. J. Pathol.* **164**, 1–7.

Yamamoto K., Yoshida H., Kokame K., Kaufman R. J. and Mori K. (2004) Differential contributions of ATF6 and XBP1 to the activation of endoplasmic reticulum stress-responsive cis-acting elements ERSE, UPRE and ERSE-II. *J. Biochem. (Tokyo)* **136**, 343–350.

Characterization of APH-1 mutants with a disrupted transmembrane GxxxG motif

Wataru Araki[1,*], Shinya Saito[1], Noriko Takahashi-Sasaki[2], Hirohisa Shiraishi[3], Hiroto Komano[3], and Kiyoko S. Murayama[1]

[1]*Department of Demyelinating Disease and Aging, National Institute of Neuroscience, NCNP, Kodaira, Tokyo 187-8502, Japan*

[2]*Department of Bioinformatics, Faculty of Engineering, Soka University, Hachioji, Tokyo 192-8577, Japan*

[3]*Department of Alzheimer's Disease Research, National Institute of Longevity Sciences, NCGG, Obu, Aichi, 474-8522, Japan*

*Corresponding author: Department of Demyelinating Disease and Aging, National Institute of Neuroscience, NCNP, 4-1-1 Ogawahigashi, Kodaira, Tokyo 187-8502, Japan. Tel.: 81-423-41-2711; Fax: 81-423-46-1747; E-mail: araki@ncnp.go.jp

Running title: Characterization of APH-1 mutants

Abstract.

APH-1 is one of the four essential components of presenilin-γ-secretase complexes. There are three major isoforms of APH-1 in humans: APH-1aS, APH-1aL, and APH-1b. To gain insight into the functional role of APH-1 in γ-secretase complexes, we analyzed the relationship between the three APH-1 forms and characterized APH-1 mutants with a disrupted transmembrane GxxxG motif. We found that overexpression of APH-1aS or APH-1b in human cells significantly reduced the levels of endogenous APH-1aL protein. However, this displacement was not observed in presenilin-deficient cells, suggesting that it is dependent on presenilin. In transiently transfected cells, the levels of APH-1aL with G122D or L123D mutations were much lower than the wild-type APH-1aL. Also, cycloheximide treatment of stable transfectants revealed that the mutant proteins are much less stable than the wild-type. Furthermore, co-immunoprecipitaion analysis showed that the wild-type but not the mutant APH-1aL is incorporated into presenilin 1 complexes, displacing endogenous APH-1aS. These results collectively indicate that the three forms of APH-1 can replace each other in presenilin complexes and that the transmembrane GxxxG region is essential for the stability of the APH-1 protein as well as the assembly of presenilin complexes.

Index entries: Alzheimer's disease; APH-1; presenilin; protein stability; γ-secretase

Introduction

Presenilin (PS) 1 and 2 have been identified as causative genes for early-onset familial Alzheimer's disease (Ephrat et al., 1995; Sherrington et al., 1995). These genes encode multipass transmembrane proteins that are essential for the γ-site cleavage of amyloid precursor protein to generate amyloid β-protein (Aβ). Mutations in PS1 and PS2 associated with familial Alzheimer's disease alter the specific location of the γ-site cleavage, increasing the level of Aβ42 relative to Aβ40 (Citron et al., 1997). The protease responsible for this cleavage, γ-secretase, is a multiprotein complex in which PS1 or PS2 act as the catalytic subunit. In this complex, PS is endoproteolysed within its hydrophilic loop to form N- and C-terminal fragments. In addition, two Asp residues in the sixth and seventh transmembrane domains comprise the active site (Sisodia and St George-Hyslop, 2002; Kimberly and Wolfe, 2003). Besides PS1 and PS2, nicastrin, APH-1, and PEN-2 have been identified as essential components of PS complexes (Yu et al., 2000; Edbauer et al., 2003; Kimberly et al., 2003; Takasugi et al., 2003), and, recently, numerous type 1 transmembrane proteins, including Notch and cadherins, have been identified as substrates of γ-secretase (Kimberly and Wolfe, 2003).

APH-1 is a seven-pass transmembrane protein that was first identified by genetic screening of *Caenorhabditis elegans* (Francis et al., 2002; Goutte et al., 2002). There are two homologues of human APH-1: APH-1a and APH-1b. Of these, APH-1a has two isoforms, APH-1aS and APH-1aL, which are generated by alternative splicing and possess different C-terminal sequences (Francis et al., 2002; Goutte et al., 2002; Lee et al., 2002; Gu et al., 2003) (Fig. 1A). We have previously shown that APH-1aS is more abundant than APH-1aL in human tissues (Saito and Araki, 2005). Several studies using RNA interference or APH-1-deficient mice have demonstrated that APH-1a is more important than APH-1b in the formation and activity of γ-secretase complexes (Lee et al.,

2002; Shirotani et al., 2004a; Ma et al., 2005; Saito and Araki, 2005; Serneels et al., 2005), but the precise reason for this difference remains unclear. APH-1 has been reported to form a subcomplex with nicastrin during the early biosynthesis of γ-secretase, and it may act as a scaffold for the assembly of the γ-secretase complex (Hu and Fortini, 2003; LaVoie et al., 2003; Morais et al., 2003; Shirotani et al., 2004b).

The mutation of Gly123 to Asp in the fourth transmembrane domain of *C. elegans* APH-1 leads to an abnormal phenotype associated with a defect in Notch signaling (Goutte et al., 2002). Gly123 is highly conserved during evolution and corresponds to Gly122 and Gly121 in mammalian APH-1a and APH-1b, respectively (Fig. 1B). Importantly, this Gly resides in a conserved transmembrane motif, GxxxG, which is a transmembrane packing motif (Russ and Engelman, 2000) that appears to be critical for the assembly and activity of the γ-secretase complex (Lee et al., 2004). In the present study, we sought to gain insights into the mechanistic role of the transmembrane GxxxG motif of APH-1, which until now has remained unclear. We found that APH-1 mutants with a disrupted GxxxG motif are highly unstable and are not incoporated into PS complexes. In addition, we found that the three forms of APH-1 can replace each other in PS complexes.

Materials and Methods

Cell culture

Human embryonic kidney 293 (HEK293) cells and HeLa cells were cultured in a humidified atmosphere of 5% CO_2/95% air at 37°C in Dulbecco's modified Eagle's medium containing 10% fetal bovine serum (Saito and Araki, 2005). The former cells were grown on collagen I-coated dishes or plates (Iwaki, Japan) to enhance adhesion. PS1/PS2-knockout and wild-type murine fibroblasts immortalized with large T antigen were maintained as previously described (Herreman et al, 2000; Shiraishi et al., 2004).

Plasmids and transfection

Human APH-1aL and APH-1aS cDNAs were prepared by reverse transcription (RT)-PCR from HEK293 cells as follows. Total RNA was extracted from cells using a Gene Elute Mammalian Total RNA Miniprep Kit (Sigma, St. Louis, MO, U.S.A.). RT was carried out in a reaction volume of 20 μl containing 1 μg total RNA and 25 μg/ml oligo(dT)15, using the ImProm II Reverse Transcription System (Promega, Mdison, WI, U.S.A.) according to the manufacturer's instructions. PCR was carried out using 1 μl RT reaction mixture in the presence of 200 μM dNTPs, 0.5 μM primers and 1 μl Advantage 2 Polymerase mix (Stratagene, La Jolla, CA. U.S.A.) in a final volume of 50 μl. PCR reaction consisted of 30 cycles of 95°C for 1 min, 65°C for 1 min, and 72°C for 2 min. The primers for APH-1aS were 5'-CTTCCCACCTGACCAGCCAT-3' and 5'-GGTGGGATCTGTCAGGCGAT-3', and the primers for APH-1aL were as described previously (Saito et al., 2005). The resulting cDNA fragments were subcloned into the pGEM-T easy vector (Promega) and sequenced with an ABI PRISM 377 DNA sequencer (PE Biosystems, Boston, MA, U.S.A.). G122D and L123D mutant APH-1aL cDNAs were generated using the QuickChange site-directed mutagenesis kit (Stratagene)

according to the manufacturer's instructions. The primers used for mutagenesis were as follows: for G122D, 5'-GATGGCCTATGTTTCTGATCTCTCCTTCGGTATCA-3' and 5'-TGATACCGAAGGAGAGATCAGAAACATAGGCCATC-3'; and for L123D, 5'-GATGGCCTATGTTTCTGGTGACTCCTTCGGTATCATCAGTG-3' and 5'-CACTGATGATACCGAAGGAGTCACCAGAAACATAGGCCATC-3'. APH-1b cDNA was subcloned as described (Saito et al., 2005).

For expression studies, these APH-1 cDNAs were inserted into the *Eco*RI site of the pcDNA3.1 vector (Invitrogen, Carlsbad, CA, U.S.A.). For transient transfections, HeLa or HEK293 cells were plated on a 6 cm-dish at a density of 5–6 × 10^5 or 1 × 10^6 cells/dish, respectively. Cells were transfected with DNA (8 μg/dish) using Lipofectamine 2000 (Invitrogen) according to the manufacturer's instructions and harvested 2 days later. For stable transfections, HEK293 cells were transfected with empty vector or wild-type or mutant APH-1aL cDNA as described above, and stable transformants were selected with 1 mg/ml G418. APH-1aS cDNA was also introduced into the *Eco*RI site of the pMX retroviral vector (to generate pMX-APH-1aS) and used to infect PS-knockout and wild-type fibroblasts as described previously (Shiraishi et al., 2004).

Antibodies

Rabbit polyclonal antibodies to APH-1aL or APH-1aS were raised against the C-terminal 21 amino acids of APH-1aL or the C-terminal 15 amino acids of APH-1aS, respectively (Fig. 1A). The anti-APH-1aL antibodies were purified on a HiTrap protein G column (Amersham Biosciences, Piscataway, NJ, U.S.A.), whereas the anti-APH-1aS antibodies were affinity purified on a HiTrap NHS-activated column (Amersham Biosciences) coupled to the peptide used for immunization. Anti-APH-1b antibodies were produced and purified as described previously (Saito et al., 2005). Rabbit polyclonal

anti-APH-1aL antibody (O2C2) and anti-nicastrin antibody were obtained from Covance (Berkely, CA, U.S.A.) and Sigma, respectively. The antibody O2C2 was sensitive enough to detect endogenous APH-1aL, but our anti-APH-1aL antibody was not. Our anti-APH-1aS antibody exhibited weak cross-reactivity with APH-1aL. Polyclonal antibodies against PS1 (αPS1-Ext1) and PS2 (Ab333) and monoclonal antibodies against PS1 (PS1N62) were described previously (Chui et al., 1998; Shirotani et al., 1999; Shirotani et al., 2000).

Western blot analysis

For Western blot analysis, cells were lysed in RIPA buffer or 1% CHAPSO buffer containing protease inhibitors (Araki et al., 2001; Saito et al., 2005). Proteins were separated on 8% or 12% SDS-PAGE, transferred to a polyvinylidene difluoride membrane, and processed as described previously (Araki et al., 2001). Protein bands were quantified using an LAS-1000 image analyzer (Fuji Film Co., Japan)

Immunoprecipitation

Cells were lysed with buffer containing 1% CHAPSO and protease inhibitors (Saito et al., 2005). The lysates were incubated with anti-PS1 antibodies (PS1N62) that had been crosslinked to protein G-agarose beads with dimethylpimelimidate, and the immunoprecipitated proteins were washed and analyzed by Western blotting with appropriate antibodies.

Cycloheximide treatment

The stable transfectants of the wild-type and mutant APH-1aL were plated on 6-cm dishes, incubated in the presence of cycloheximide (100 μg/ml) for up to 12 h, and

analyzed by Western blotting with the anti-APH-1aL antibody.

Results

To investigate the relationship among the three forms of APH-1, we transiently transfected HEK293 and HeLa cells with APH-1aS or APH-1b and examined the expression of endogenous APH-1aL by Western blotting with the anti-APH-1aL antibody (O2C2). As shown in Fig. 2A, overexpression of APH-1aS (~22 kDa) or APH-1b (~25 kDa) reduced the endogenous expression of APH-1aL (~24 kDa) in both cell lines. We noted that APH-1aS had a slightly more significant effect than APH-1b. Similar results were observed in HEK293 cells stably expressing APH-1aS and APH-1b (data not shown). In both HeLa and HEK293 cells, the displacement effect of APH-1aS on endogenous APH-1aL appeared to be dependent on the level of APH-1aS expression (Fig. 2B and data not shown).

As this effect is reminiscent of the replacement effect between PS1 and PS2 (Thinakaran et al., 1996), we surmised that the displacement is due to competition among the three forms of APH-1 for their binding partners during the formation of PS complexes. To explore this possibility, we overexpressed APH-1aS in fibroblasts derived from PS1/PS2-deficient or wild-type mice by retrovirus-mediated expression and then examined the levels of endogenous APH-1aL. As shown in Fig. 2C, we observed significantly reduced APH-1aL levels in APH-1aS-transfected wild-type fibroblasts compared with mock-transfected cells. In contrast, endogenous APH-1aL levels were unaltered in APH-1aS-transfected PS-null cells compared with mock-transfected cells, although the APH-1aL levels were much lower in PS-null cells than in wild-type cells (Fig. 2C). These results show that the displacement of endogenous APH-1aL by overexpressed APH-1aS does not occur in the absence of PSs, suggesting that the effect is PS-dependent. Interestingly, the levels of immature nicastrin were augmented by exogenous APH-1aS not only in PS-null cells but also wild-type cells, suggesting a

stabilizing effect of APH-1aS on immature nicastrin.

To clarify the physiological role of the GxxxG motif in the fourth transmembrane domain of APH-1 (Fig. 1B), we generated two mutant APH-1aL constructs in which the conserved Gly122 or Leu123 is substituted by Asp (G122D or L123D APH-1aL) and then transiently expressed them or wild-type APH-1aL in HEK293 and HeLa cells. Surprisingly, Western blotting revealed that the levels of both APH-1aL mutants were much lower than those of wild-type APH-1aL in both cell lines (Fig. 3A). It should be noted that we used our APH-1aL antibody, which can detect only overexpressed Aph-1aL in these experiments. Quantitative analysis further revealed that the expression levels of G122D APH-1aL and L123D APH-1aL were approximately 40% of the wild-type APH-1aL (Fig. 3B).

These results suggest that the lower expression of the mutant APH-1aL proteins is due to their instability. To evaluate the stability of the mutant APH-1aL proteins, we generated HEK293 cell lines stably expressing equivalent levels of wild-type and G122D mutant APH-1aL (designated WT-APH-1aL and GD-APH-1aL cells, respectively; Fig. 4A). Following cycloheximide blockade of protein synthesis, we assessed the levels of overexpressed APH-1aL in these cells. As shown in Fig. 4A, the G122D mutant APH-1aL appeared to be more unstable than the wild-type protein; Fig. 4B reveals that the half-life of the mutant was 6.1 h, which was about half that of the wild-type (11.9 h).

To further clarify the mechanism underlying the instability of the mutant APH-1aL, we examined the co-immunoprecipitation of APH-1 proteins and endogenous PS1. CHAPSO extracts of control vector-transfected cells, WT-APH-1aL cells, and GD-APH-1aL cells were immunoprecipitated with anti-PS1 antibodies and then analyzed by Western blotting with anti-APH-1aL antibodies. Approximately 2-fold more APH-1aL protein associated with PS1 in WT-APH-1aL cells than in control cells, whereas the amounts of

PS1-associated APH-1aL were almost unaltered in GD-APH-1aL cells (Figs. 5A, B). This result clearly indicates that wild-type APH-1aL, but not the mutant, was incorporated into PS1 complexes. We also found that the levels of endogenous APH-1aS proteins associated with PS1 were much lower (approximately one-third) in WT-APH-1aL cells than in control cells, but they were almost unchanged in GD-APH-1aL cells (Figs. 5A, B). Thus, endogenous APH-1aS was displaced by wild-type APH-1aL but not by G122D mutant APH-1aL. In addition, the levels of endogenous PS1 were almost equivalent in these cells (Fig. 5A). Endogenous APH-1b, however, could not be detected with our anti-APH-1b antibody. Furthermore, we confirmed that nicastrin and PEN-2 co-precipitated with PS1 (data not shown). Taken together, the present results indicate that mutant APH-1aL proteins with a disrupted GxxxG motif are highly unstable and are not incorporated into PS complexes.

Discussion

Recent results have suggested that there are at least six distinct PS complexes because the three APH-1 isoforms (APH-1aS, APH-1aL, and APH-1b) seem to be independently incorporated into either PS1 complexes or PS2 complexes (Sebastien et al., 2004; Shirotani et al., 2004a). However, it is not yet clear whether APH-1a- and APH-1b-containing complexes have different functions as γ-secretases or how these complexes are related to each other. In this study, we showed that exogenous APH-1aS downregulates endogenous expression of APH-1aL in a dose-dependent manner and that exogenous APH-1b has a similar but weaker effect. We used PS-deficient fibroblasts to show that such displacement of endogenous APH-1aL does not occur in the absence of PSs. These results suggest that the displacement occurs because APH-1aS, APH-1aL, and APH-1b compete for common binding partners to form PS complexes (Gu et al., 2003) and that the three forms can replace each other. APH-1aL appears to be more readily replaced with APH-1aS than APH-1b, probably because of their structural similarity. It should also be noted that displacement of one form of APH-1 by the overexpression of another can be an indicator of the incorporation of the overexpressed APH-1 into PS complexes.

The G122D mutation, which was first found in a loss of function mutant of *C. elegans* APH-1, likely disrupts the conserved GxxxG motif in the fourth transmembrane domain of APH-1 (Lee et al., 2004). Although this motif is generally considered to be important in mediating high-affinity association of transmembrane helices (Russ and Engelman, 2000), it also appears to be important for the assembly of PS complexes (Lee et al., 2004). We found that, upon transient expression, the levels of two mutants of APH-1aL (G122D and L123D) were much lower than that of wild-type APH-1aL. We also compared the stability of the wild-type and G122D mutant APH-1aL proteins in

stably transfected cells treated with cycloheximide. Our results clearly indicate that the G122D mutant protein is much less stable than the wild-type protein, in agreement with the findings of a recent study in *Drosophila* cells (Niimura et al., 2005). We found that the half-life of overexpressed wild-type APH-1 is 11.9 h in HEK293 cells. Our results do not appear to support the idea that APH-1 is a highly stable protein (Niimura et al., 2005), because the half-life is only 12 h.

Our co-immunoprecipitation analyses confirmed that the G122D mutant of APH-1aL neither incorporates into PS1 complexes nor displaces endogenous APH-1aS. This is consistent with previous reports indicating that this Gly mutant of APH-1 does not physically associate with PS1 (Edbauer et al., 2004; Lee et al., 2004; Niimura et al., 2005). On the basis of our present findings, we propose a simplified model (Fig. 6) wherein wild-type APH-1aL interacts with PSs and is stabilized and incorporated into mature PS complexes, resulting in displacement of endogenous APH-1aS. In contrast, the G122D mutant APH-1aL does not interact with PSs and does not participate in PS complexes, resulting in its rapid degradation. It should be noted that, unlike previous studies (Edbauer et al., 2004; Lee et al., 2004; Niimura et al., 2005), we used untagged APH-1 rather than C-terminally tagged APH-1 because the untagged form is expected to enable a more accurate assessment of the mutant APH-1 protein.

Our data suggest that not only Gly122 but also Leu123 are important for the integrity of the GxxxG region. These results are consistent with the fact that the GxxxG pair frequently occurs adjacent to bulky residues such as Val and Leu (Russ and Engelman, 2000). Although the GxxxG sequence is likely to mediate docking or packing of APH-1, it is not clear whether the region directly interacts with PSs or is involved in the intermolecular or intramolecular interactions of APH-1 molecules themselves (Lee wt al., 2004; Niimura et al., 2005). Intriguingly, however, PS1 and PS2 have a conserved